BIOCHEMISTRY

 Volume 45, Number 41 October 17, 2006

Accelerated Publications

On the Seeding and Oligomerization of pGlu-Amyloid Peptides (*in vitro*)

Stephan Schilling,[‡] Thomas Lauber,[§] Michael Schaupp,[§] Susanne Manhart,[‡] Eike Scheel,[‡] Gerald Böhm,[§] and Hans-Ulrich Demuth*,[‡]

Probiodrug AG, and ACGT ProGenomics AG, Weinbergweg 22, 06120 Halle/Saale, Germany

Received June 25, 2006; Revised Manuscript Received August 22, 2006

ABSTRACT: Oligomerization of amyloid β (Aβ) peptides is the decisive event in the development of Alzheimer's disease (AD), the most common neurogenerative disorder in developed countries. Recent evidence links this conformation-driven process to primary- and secondary-structure modifications of Aβ. The N and C terminus of deposited Aβ has been shown to possess conspicuous heterogeneity. While the C-terminally longer form of Aβ, i.e., Aβ (42), is considered more amyloidogenic, the role of the N-terminal modifications, e.g., truncation and glutamate cyclization accounting for the majority of the deposited peptides, is less understood. In the present study, we characterized the oligomerization and seeding capacity of pGlu-amyloid peptides using two unrelated techniques based on flow cytometry or flourescence dye binding. Under different conditions and irrespective of the C terminus of Aβ, i.e., Aβ40 or 42, pGlu-modified peptides displayed an up to 250-fold accelerated initial formation of aggregates compared to unmodified Aβ. The accelerated seed formation is accompanied by a change in the oligomerization kinetics because of N-terminal pGlu formation. Furthermore, the formation of mixed aggregates consisting of either pGlu-Aβ (3−42) or ADan or ABri and Aβ (1−42) was investigated by Aβ fluorescence labeling in flow cytometry. The results suggest that pGlu-modified peptides are potential seeding species of aggregate formation *in vivo*. The data presented here and the abundance of pGlu peptides in amyloidoses, such as FBD and AD, suggest pGlu-amyloid peptides as a species with biophysical characteristics that might be in particular crucial for the initiation of the disease.

Amyloid β (Aβ)[1] peptides, generated by proteolytic processing of the large class one transmembrane protein, amyloid precursor protein (APP), are the major protein components of neuritic plaques in sporadic and familial Alzheimer's disease (AD) (*1*, *2*). Cleavage of APP by the protein complex γ-secretase leads to the formation of the C terminus and either Aβ40 or 42. In particular, the longer Aβ species display a pronounced amyloidogeneity, and increased generation of Aβ42 inevitably leads to the development of AD (*3*−*6*). Moreover, it has been shown that amyloid deposits in humans and animal models of AD are mainly composed of Aβ42 that is required and sufficient for plaque formation (*7*).

Analysis of neuritic and vascular plaques of AD patients, however, also revealed a prominent N-terminal heterogeneity of Aβ. Besides Aβ(11−40/42), which is generated by the β'-cleavage of APP by β-secretase (BACE), peptides are deposited displaying a racemized or isomerized aspartic acid at positions 1 and 7 (*8*−*10*). Furthermore, N-truncated amyloid peptides have been identified as a major component in many familial AD (FAD) cases (*11*). Among these

* To whom correspondence should be addressed: Probiodrug AG, Weinbergweg 22, 06120 Halle, Germany. Telephone: +49-345-5559900. Fax: +49-345-5559901. E-mail: hans-ulrich.demuth@probiodrug.de.

[‡] Probiodrug AG.

[§] ACGT ProGenomics AG.

[1] Abbreviations: Aβ, amyloid β; AD, Alzheimer's disease; APP, amyloid precursor protein; FAD, familial AD.

10.1021/bi0612667 CCC: $33.50
Published on Web 09/20/2006

peptides, the most prominent forms have been identified to start at position 3 or 11 possessing N-terminal pyroglutamic acid, which is generated from glutamic acid (*9*, *12*−*16*).

Pyroglutamyl formation from N-terminal glutamine is a well-established protein modification, which is catalyzed by glutaminyl cyclase (*17*, *18*). Recently, however, we were able to demonstrate that glutaminyl cyclase converts also N-terminal glutamyl residues, thus making the enzyme a potential catalyst of pGlu-Aβ formation (*19*).

Several initial studies suggest that the pGlu-Aβ species, i.e., pGlu-Aβ(3−40/42) and pGlu-Aβ(11−40/42) play a crucial role in the development of AD: (i) the pGlu residue stabilizes the peptides against degradation by aminopeptidases; (ii) they appear very early in the disease process; and (iii) pGlu-Aβ peptides displayed an enhanced cytotoxicity (*14*, *20*−*22*). Most interestingly, however, a recent study revealed differences in the composition of amyloid plaques between patients suffering from AD and healthy aged individuals. The major difference in the Aβ deposits was an obvious abundance of pGlu-Aβ species in the case of AD, indicating a decisive role of pGlu-Aβ for the development of the disease (*23*).

It was the aim of the present study to characterize the nucleation characteristics of pGlu-Aβ peptides in more detail and to compare the propensity of oligomerization with the full-length and N-truncated amyloid peptides to provide evidence for the pronounced deposition in amyloid plaques.

MATERIALS AND METHODS

Materials. Aβ peptides were synthesized as described below or purchased from Bachem (Bubendorf, Switzerland) or AnaSpec (San Jose, CA). Thioflavin T (ThT) was obtained from Fluka (Buchs, Switzerland). All other chemicals, e.g., high-performance liquid chromatography (HPLC) solvents, were of analytical grade.

Synthesis and Purification of Aβ Peptides. Peptides were synthesized in 50 μmol scale on Fmoc-Val/Ala-NovaSyn-TGA resin (0.15 mmol/g) using an automated Symphony Synthesizer (Rainin). Briefly, Fmoc amino acids (5-fold excess, double couplings) were activated with equimolar amounts of TBTU/NMM in *N*,*N*-dimethylformamide (DMF). Fmoc deprotection was done by 20% piperidine in DMF. Fmoc-Gly-Ser(ΨMe,Mepro)-OH was introduced instead of Gly25-Ser26 to disrupt the aggregation of the peptide chain. Global cleavage and deprotection was carried out by using a mixture of TFA/EDT/TIS/water (94:2.5:2.5:1) for 4 h. The crude peptides were dissolved in HFIP for preparative HPLC. Preparative HPLC was performed with a gradient of solvent B (60% acetonitrile and 40% solvent A) in solvent A [0.1% NH_4OH in H_2O at pH 9.0]: 10% B for 2 min and 10−100% B until 35 min on a 250 × 10 Gemini C18 column, 10 μm (Phenomenex). Prior to labeling, all Aβ peptides were treated as reported previously (*24*) to obtain seedless material and further purified by RP-HPLC (column, Source 5RPC 4.6/150 ST (Amersham); solvent A, 0.1% NH_4OH in H_2O at pH 9.0; solvent B, 60% acetonitrile and 40% solvent A; gradient, 25−56% solvent B in 31 min; flow rate, 1.0 mL/min) and lyophilized. Peptide purity and identity were confirmed by analytical HPLC (150 × 4.6, 5μ Source or Gemini) and matrix-assisted laser desorption ionization mass spectroscopy (MALDI−MS).

Synthesis and Purification of ADan and ABri. ADan and ABri were synthesized as described above for Aβ peptides. Fmoc-Glu-Thr(ΨMe,Mepro)-OH was introduced instead of Glu18-Thr19. Preparative HPLC was performed applying a gradient of acetonitrile in water (20−95% acetonitrile and 0.04% TFA over 40 min) on a 250 × 21.2 Luna C18(2) column, 10 μm (Phenomenex). Peptide purity and identity were confirmed by analytical HPLC [125 × 4.0, 5μ Luna C18(2)] and MALDI−MS.

Fluorescence Labeling. The peptides Aβ (1−42), Aβ (3−42), and pGlu-Aβ (3−42) were labeled with the fluorescence dye Alexa Fluor 488 according to the instructions of the manufacturer (Alexa Fluor 488 5-TFP; Invitrogen). The different reaction products were then separated by RP-HPLC as described above, analyzed by HPLC−MS, and lyophilized in the dark. The content of each peptide was determined by amino acid analysis (ZPA Bingen, Germany). The anti-Aβ antibody 4G8 (Chemicon International) was labeled with the fluorescence dye Alexa Fluor 488 according to the instructions of the manufacturer (Alexa Fluor 488 monoclonal antibody labeling kit; Invitrogen). Primary amino groups are subjected to derivatization by the fluorescent dye, i.e., the primary amino groups and the lysyl side chains. The reaction mixture was subjected to separation using HPLC, applying the method that was described in the synthesis section. The fractions were analyzed using mass spectrometry, to identify the degree of labeling. For the assays, only single- and double-labeled peptides were applied.

Preparation of Seedless Aβ Stock Solutions. Prior to analysis, the lyophilized amyloid peptides were subjected to a disaggregation procedure (*24*). The peptides were dissolved in HFIP (1.0 mM) and evaporated in a stream of nitrogen. Residual solvent was removed by evacuation in a speed vac for 10 min. Afterward, stock solutions of Aβ42 (100 μM) and Aβ40 (5 mM), were prepared in pure dimethyl sulfoxide (DMSO). Aβ solutions treated in this way have been described to be free of oligomeric species (*39*).

Aggregation Assay and Flow Cytometry. Seedless Aβ peptides were diluted to 10 μM (final total peptide concentration) in 50 mM sodium acetate at pH 5.5 containing 2 mM DTT and 100 mM NaCl and incubated at 37 °C without shaking. For fibril formation analysis, the peptides were either used as a mixture of unlabeled peptide (80%) and the respective fluorescence-labeled peptide (20%) or as unlabeled peptides alone. For the seeded aggregation, each reaction contained 70% unlabeled Aβ (1−42), 20% Alexa Fluor 488 labeled Aβ (1−42), and 10% of either unlabeled peptide pGlu-Aβ (3−42), ADan, or ABri. To characterize the progress of the reaction, aliquots were removed at the indicated times, diluted to 10 nM in phosphate-buffered saline (PBS)-T (0.05% Tween-20) and analyzed. For reactions containing unlabeled peptides only, prior to flow cytometry, aliquots were diluted to 5 nM in PBS-T and incubated with fluorescence-labeled antibody 4G8 at 1 nM for 1 h at 4 °C.

For the detection of Aβ oligomers and fibrils produced during solution-phase aggregation, a Cytomics FC500 (Beckman Coulter) flow cytometer equipped with a single 20 mW 488 nm argon-ion laser was used. The green fluorescence of the dye Alexa Fluor 488 was detected by the corresponding FL1 (logarithmic scale) photomultiplier equipped with a 525 bandpass filter. To ensure identical conditions for all

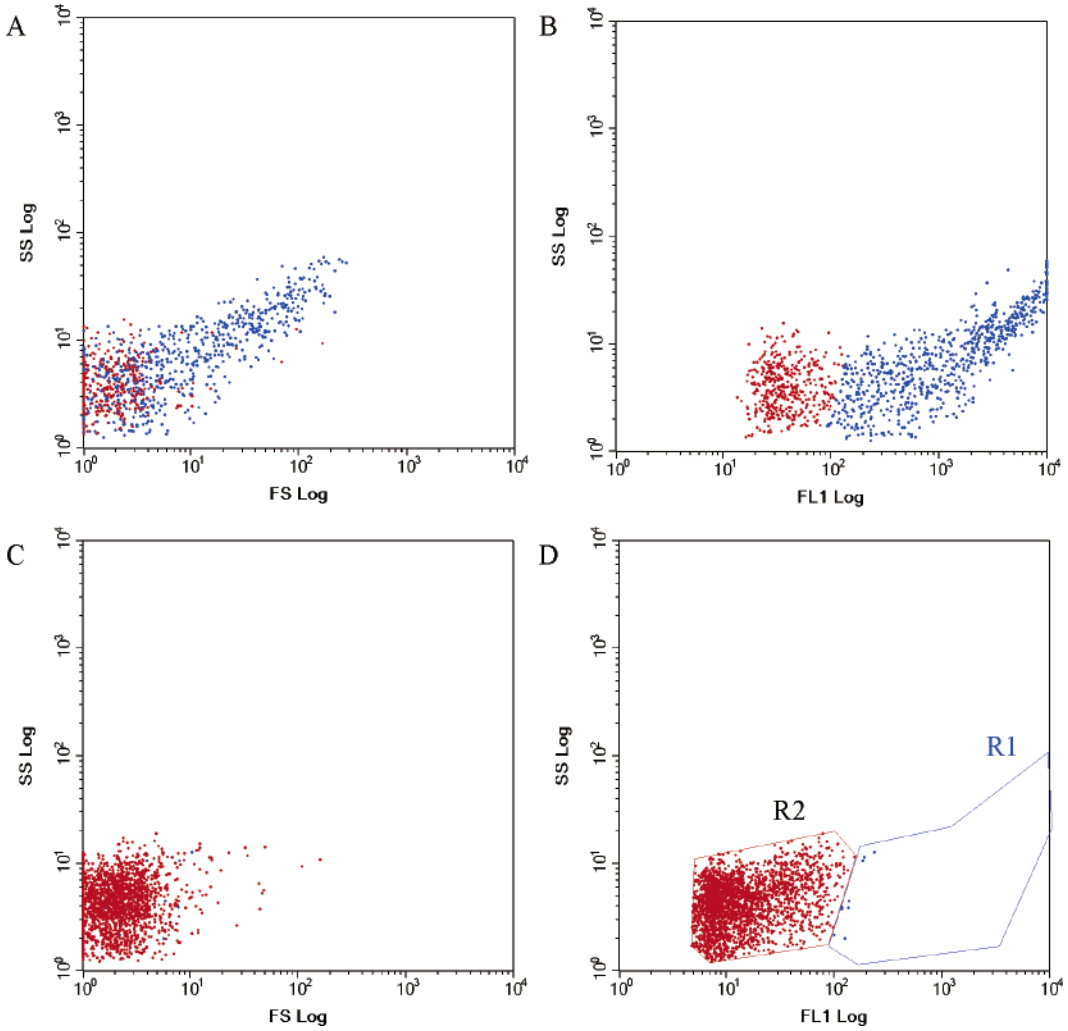

FIGURE 1: Detection of *in vitro* assembled Aβ fibrils (A and B) and oligomers (C and D) by flow cytometry. FS log, forward scatter; SS log, side scatter; and FL1 log, fluorescence 1 channel. The different size distributions (FS log/SS log dot blots) of fibrils (A) and oligomers (C) correlate with the signal intensity in the FL1 channel (B and D; regions R1 and R2) and allow for a differentiation of these structures in a single experiment. It should be noted that the assay does not detect any monomeric species; i.e., at time point 0, after the reaction starts, no signal can be observed, which also becomes evident from the data displayed in Figures 2 and 3.

measurements, all samples were measured in TruCount Tubes (BD Biosciences) and analysis was stopped after 20 000 beads were counted. Counts were transferred into Alzheimer-normalized specific measurement signal (ANSMS) for evaluation: event counts from flow cytometry analysis normalized to the size of the particles, i.e., to a mean size of FS log = 250. Because there is a correlation between particle size (FS log in parts A and C of Figure 1) and intensity of the fluorescence signal (FL1 log in parts B and D of Figure 1), we were able to discriminate between smaller oligomeric and larger fibrillar structures in a single experiment. Thus, different regions in a FL1 log/SS log dot blot comprising areas of strong or weak fluorescence intensity were assigned to fibrils or oligomers, respectively (regions R1 and R2 in parts B and D of Figure 1).

ThT Assay. Fibril formation analysis using ThT fluorescence was performed essentially as described previously (*25*). The DMSO stock solution was diluted in PBS to a final concentration of 50 μM Aβ peptide. The peptide solution was added to an equal volume of ThT solution (20 μM ThT, 0.3 M NaCl, and 0.01% NaN_3) and applied to a 96-well microplate. Routinely, assays of each peptide were performed in triplicate on one plate. The plate was covered with an adhesive film (EXCEL Scientific, Wrightwood, CA) and incubated in the plate reader at 30 °C for up to 250 h. The fluorescence was measured every 4 h (excitation, 440 nm; emission, 590 nm).

Data Evaluation. Aβ data were analyzed according to common algorithms (*26*). Fibril formation from monomeric Aβ was evaluated using eq A

$$y = \text{limit}[1 - 1/(1 + e^{at+b})] \quad \text{(A)}$$

The progress curve of the *de novo* pGlu-Aβ (3−40) fibril formation was analyzed according to eq B, denoting a quick initial first-order aggregation reaction, which is followed by a higher order fibril formation process

$$y = \text{limit1} - e^{-at+b} + \text{limit2}[1 - 1/(1 + e^{ct+d})] \quad \text{(B)}$$

The velocity of the initial seed formation was quantified from the derivatives in respect to time

$$y' = (\text{limit}ae^{at+b})/(1 + e^{at+b})^2 \quad \text{(A}'\text{)}$$

and

$$y' = ae^{-at+b} + (\text{limit2}ce^{ct+d})/(1 + e^{ct+d})^2 \qquad (B')$$

RESULTS

Aβ42 Oligomerization/Fibril Formation. Oligomerization of Aβ42 variants was evaluated using solution-state aggregation and a new flow-cytometry-based assay (further details will be published elsewhere: Santos et al. Detection of amyloid-β oligomers in human cerebrospinal fluid by flow cytometry. A new diagnostic tool for Alzheimer's disease, manuscript in preparation). Native Aβ42 was spiked with its monomeric Alexa Fluor 488 labeled counterpart (20% of the final concentration) and incubated at a 10 μM total peptide concentration for up to 24 h (Figure 2). At indicated times, samples were removed, diluted to 10 nM (on the basis of the initial concentration of the monomer), and analyzed. As illustrated in Figure 2A, only very little fibril formation was detected for Aβ (1−42) after 24 h of incubation. Apparently, the characteristic lag phase spans the first 20 h, which is indicative of a slow formation of seeds that are required for fibril elongation. In contrast, the samples containing the N-truncated variants Aβ (3−42) and pGlu-Aβ (3−42) displayed fibril formation already after a few hours, and seed fibril formation appeared to be complete after 24 h. Most interestingly, fibril formation from monomeric pGlu-Aβ (3−42) was finished already after 2−3 h of incubation, implying an exceptionally high tendency toward aggregation.

The data were verified for Aβ (1−42) and pGlu-Aβ (3−42) by another set of experiments using unmodified Aβ peptides and an incubation with a fluorescence-labeled antibody (clone 4G8) prior to analysis by flow cytometry. As observed with the labeled peptides, fibril formation was virtually finished in the case of pGlu-Aβ (3−42) after 1 h of incubation (Figure 2B). During the time course of the experiment, only minor fibril formation was detected for Aβ (1−42). After 24 h, however, the fibril concentration appeared to be the same as in the case of pGlu-Aβ (3−42). Altogether, pGlu-Aβ (3−42) aggregated 17−250 times faster than Aβ (1−42), depending upon the assay method (Table 1).

Influence of pGlu-Aβ (3−42), ADan, and ABri on the Fibril Formation of Aβ (1−42). On the basis of the results obtained with the monomeric Aβ, another experimental approach was undertaken to characterize the potential role of N-truncated, modified Aβ for the formation of aggregates. Monomeric pGlu-Aβ (3−42) was incubated with labeled Aβ (1−42) and unmodified Aβ (1−42) at a 10 μM final peptide concentration and a relative ratio of 1:2:7, respectively (Figure 3A). Interestingly, fibril formation was detected after 4−5 h in the presence of pGlu-Aβ (3−42). This contrasts with the significantly longer lag phase observed with Aβ (1−42) alone, indicating that the addition of pGlu-Aβ to Aβ (1−42) leads to accelerated seeding of the fibril formation of the excess of Aβ (1−42), implying, in turn, that N-truncated and full-length Aβ form mixed fibrillar aggregates.

Additionally, *de novo* fibril formation of monomeric Aβ (1−42) was assessed in the presence of two other pGlu-amyloid peptides, ADan and ABri. ADan has been identified to form deposits in conjunction with Aβ42 in FDD (*37*). Intriguingly, the formation of fluorescent aggregates was massively accelerated by both peptides (Figure 3B). Thus,

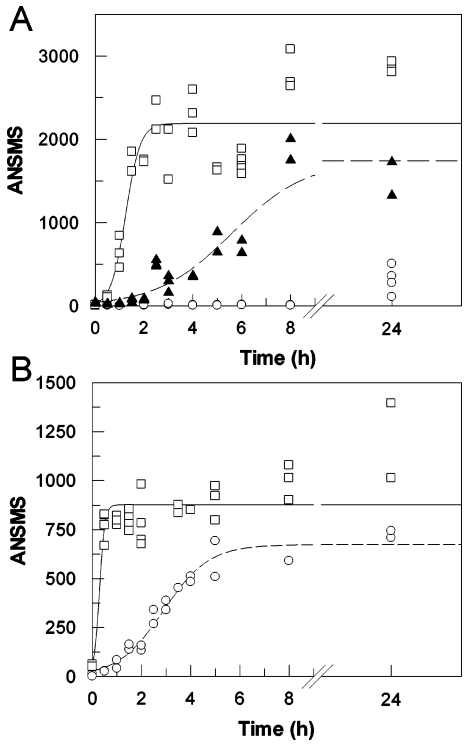

FIGURE 2: Fibril formation from monomeric Aβ (1−42) (○), Aβ (3−42) (▲), and pGlu-Aβ (3−42) (□) analyzed using flow cytometry. (A) Fibril formation from a mixture of unlabeled (80%) and Alexa Fluor 488 labeled (20%) Aβ peptides analyzed as shown in Figure 1. (B) Fibril formation from unlabeled Aβ peptides followed by incubation with a labeled 4G8 antibody and analysis using flow cytometry. With unlabeled peptides, the fibril formation was more rapid, suggesting a little influence of the direct labeling on fibril formation. In both evaluations, however, N-truncated peptides aggregated more rapidly compared to Aβ (1−42).

Table 1: Initial Velocities of Aggregate Formation, Determined from the Kinetic Analysis (Figures 2−4)[a]

		labeled	unlabeled
	pGlu(3−42)	105	481
Aβ**42**[b]	3−42	29	
	1−42	0.4 (2.5,[c] 16[d])	28
	pGlu(3−40)		4.2
Aβ**40**[e]	3−42		0.26
	1−42		0.025

[a] Labeled and unlabeled refers to the method of aggregate detection. For experimental conditions, please see the Materials and Methods. [b] ANSMS/h. [c] In presence of 10% pGlu(3−42). [d] In presence of 10% ABri. [e] RFU/h.

the differences observed in the fibril formation of Aβ (1−42) in the presence of pGlu peptides appear to be mediated by an initial seed formation of pGlu peptide, generating a nidus for the Aβ (1−42) oligomerization. It should be noted, in this respect, that the aggregation of the pGlu species itself was not observed because only Aβ (1−42) was fluorescence-labeled in the experimental settings. According to the data in Table 1, seeding of the Aβ (1−42) aggregation by either pGlu-Aβ (3−42) or ABri enhances Aβ (1−42) oligomerization by a factor of about 6 and 40, respectively.

Aβ40 Fibril Formation. To substantiate the observations for the Aβ42 peptides, the fibril formation of different Aβ40 species was analyzed using a common ThT fluorescence assay (*25*). Stock solutions of Aβ (1−40), Aβ (3−40), and pGlu-Aβ (3−40) in HFIP were prepared as described,

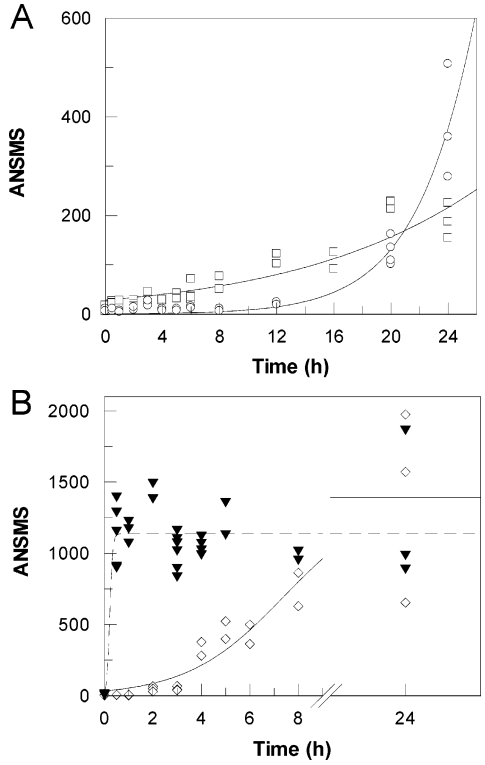

FIGURE 3: Fibril formation from monomeric Aβ (1−42), triggered by different seeding species. (A) Comparison of monomeric Aβ (1−42) (80% unlabeled and 20% Alexa-Fluor labeled) (○) with a sample consisting of 70% monomeric unlabeled Aβ (1−42), 20% monomeric Alexa-Fluor labeled Aβ (1−42), and 10% monomeric unlabeled pGlu-Aβ (3−42) (□). (B) Aβ (1−42) fibril formation is triggered by the pGlu peptides ADan (▼) and ABri (◇). Initial aggregate formation is accelerated by the addition of the peptides, as indicated by the shorter lag times. The detection mode (fluorescence) implies a formation of mixed aggregates.

evaporated, and dissolved in DMSO. Stock solutions of Aβ were diluted in PBS, and a ThT solution was added and applied to a microplate at a final concentration of 25 and 10 μM, respectively. A set of typical progress curves are illustrated in Figure 4. As observed for the Aβ42 peptides before, the N-truncated Aβ40 species showed an earlier raise in fluorescence compared to Aβ (1−40), indicating an accelerated initial ThT-positive aggregate formation. Interestingly, pGlu-Aβ (3−40) displayed a much faster aggregation compared to the noncyclized counterpart, suggesting an influence of the N-terminal modification on the fibril formation, in particular on the seeding process. Very similar progress curves of the ThT-mediated visualization of the aggregation process were observed for Aβ (11−40) and pGlu-Aβ (11−40) (not shown). Moreover, in the case of the pGlu-Aβ40 peptides, the progress curves revealed a different shape compared to the N-truncated, unmodified peptides. The typical lag phase, i.e., the thermodynamically unfavorable period, in which the seeds are generated, is displaced by a hyperbolic initial phase. Thus, the pGlu residue apparently provokes differences in fibril formation. Obviously, there is a much higher tendency toward the formation of ThT-positive initial aggregates. In contrast, the N-truncated Aβ40 variants displayed a prolonged time to reach the maximum fluorescence, indicating a slower fibril elongation. The maximum values, however, were very similar, substantiating a virtually identical ThT load and equal Aβ concentrations.

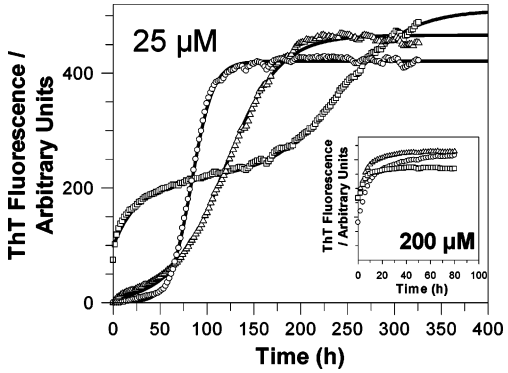

FIGURE 4: Kinetics of aggregation of Aβ (1−40) (○), Aβ (3−40) (△), and pGlu-Aβ (3−40) (□) monitored by ThT fluorescence. For pGlu-Aβ (3−40), an initial lag phase was not observed under the applied conditions, indicating an influence of the pGlu residue on the formation of seeds. Therefore, eq A, which reflects the fibril formation of Aβ (3−40) and Aβ (1−40) well, was modified by an initial exponential phase (eq B) to fit with the kinetic data of pGlu-Aβ (3−40) aggregation. At a 200 μM concentration, the initial lag phase was not observed for all peptides (inset). The overall similar final fluorescence intensity implies a comparable ThT-binding capacity of the aggregates.

In comparison to the initial velocity of the apparent fibril formation (Figures 2 and 4), it becomes in general clear that pGlu-Aβ forms conglomerates fastest, while Aβ(1−40/42) aggregate much slower. These results conform with the qualitatively observed accelerated oligomerization of Aβ (1−42) versus Aβ (1−40) (*21*, *27*). However, the enormous oligomerization capacity of pGlu-Aβ was not expected. In comparison to specifically the oligomerization of the investigated C-terminally different Aβ peptides, aggregation of the Aβ (40) peptides proceeds about 100 times slower than that of the corresponding Aβ (42) peptides. Interestingly, similar to the Aβ (42) peptides, both N-terminally truncated peptides pGlu-Aβ (3−40) and Aβ (3−40) aggregate faster (170 and 17 times, respectively) than Aβ (1−40) (Table 1).

All of these results conform with previous qualitatively observed accelerated oligomerization of full-length Aβ (1−42) versus Aβ (1−40) (*21*, *27*). However, neither the enormous oligomerization capacity of pGlu-Aβ nor that of ADan observed here was anticipated.

DISCUSSION

Recent studies on the structure of Aβ aggregates using solid-state NMR and isotope exchange generated insights into the interactions of the molecules in the fibrillar state (*28*−*31*). Apparently, the regions between residues 11 and 25 and residue 28 to the C-terminal end form a parallel β strand, which is stabilized by intramolecular hydrogen bonds. In these studies, the N-terminal amino acids, however, are solvent-accessible and structurally disordered. Furthermore, fibril formation triggered within short internal sequences lacking the N-terminal amino acids of Aβ, e.g., Aβ (15−23) or Aβ (25−35), has been well-established (*32*−*34*). Thus, one could argue that N-terminal-truncated and modified peptides that are abundant in amyloid deposits of AD brains do not reveal significant changes in the aggregation behavior. Evidence, however, for a potential influence of the N-terminus on the sedimentation of Aβ40/42, was already previously mentioned (*21*, *33*). In the present study, we performed an extended kinetic analysis of oligomerization

of N-terminal-truncated and pyroglutamyl-modified peptides with an emphasis on the physiological abundance of either species, i.e., on the Aβ(1−40/42), pGlu-Aβ(3−40/42), and the noncyclized counterparts Aβ(3−40/42) (*8*, *9*, *14*−*16*, *23*), applying flow cytometry and ThT-binding assays. Using these independent techniques, a significant influence of N-terminal truncation in general but of N-terminal pGlu formation in particular on the aggregation of Aβ was observed. The effect appeared to be more evident for the Aβ42 species compared to Aβ40. The fibril formation of pGlu-Aβ peptides was generally characterized by a short if any lag time. This, in turn, implies that the formation of seeds that are required for fibril elongation is very rapid compared to the N-terminally unmodified species. The latter is substantiated by a comparison of the initial velocities of aggregate formation, which reveals a 50−200-fold faster oligomerization of pGlu-Aβ peptides compared to Aβ(1−40/42) (Table 1).

One reason for the accelerated seed formation might be the loss of the three charged, hydrophilic groups because of N-truncation and cyclization generating a blocked N terminus. Because of modification, the hindrance for conformational changes leading to the intramolecular β sheet might be reduced, resulting in aggregate formation. This is also corroborated by the higher propensity of pGlu-amyloid peptides to form a β-sheet structure as evidenced by CD spectroscopy (*21*). Moreover, it has been described that conformational constraints, e.g., by introduction of an intramolecular lactam, may lead to a massively accelerated aggregation of Aβ because of the enforcement of a conformation that is highly prone to aggregation (*30*). Similarly, the N-terminal truncation and subsequent modification might accelerate the constructive assembly of Aβ molecules by reducing other competing conformational states.

The accelerated formation of initial seeds by N-terminally modified Aβ peptides suggests that these species are initiators of Aβ deposition and later plaque formation by N-terminally intact Aβ molecules. As expected from the structural studies that revealed the major contribution of the C-terminal part of Aβ toward the stabilization of ordered aggregates, the N-terminal variants form mixed fibrils as evidenced by the acceleration of Aβ (1−42) fibril formation by monomeric pGlu-Aβ (3−42) (Figure 3). This process might mimic the formation of initial Aβ aggregates *in vivo*. Such consideration is supported by several lines of evidence: (i) N-terminally truncated and pGlu-modified peptides constitute the majority in diffuse plaques (*8*, *16*); (ii) the C-terminal fragments of APP after cleavage by β-secretase display N-terminal pGlu formation, indicating that modification occurs prior to Aβ formation, possibly intracellularly (*13*); and (iii) in the brain of patients suffering from FAD, a massive accumulation of N-truncated and modified peptides was observed, suggesting a decisive role of these species for the development of the disease (*11*, *35*). The latter was also corroborated by a recent study, in which the amyloid plaque composition of the brain from patients suffering from sporadic AD and normal aged individuals was compared, revealing an over-representation of pGlu-Aβ peptides in the case of AD. Thus, possibly because of the increased amyloidogeneity, N-truncated and modified peptides influence, likely, the speed of the development of the disease (*36*, *37*). Moreover, the N-terminal pyroglutamyl formation renders the peptides resistant toward degradation by aminopeptidases, which is assumed to be one potential way of degradation of Aβ in the brain (*38*). Thus, pyroglutamyl formation marks an endpoint for degradation directed on the N terminus, which further favors the aggregation of pGlu-Aβ peptides relative to the slower aggregation of full-length Aβ, which is also subject to intense proteolysis.

In conclusion, N-terminal truncation in general but N-terminal pyroglutamyl formation in particular might be important for initial events leading to the development of Alzheimer's pathology. This is especially emphasized by the increased amyloidogeneity and seeding capacity of the modified Aβ peptide, which is demonstrated in this study. It is tempting at this point to speculate that perhaps the extraordinary seeding and self-seeding capacity of ADan and ABri observed in our study might be related to the pathophysiological particularly fast disease progression in FDD or FBD.

Therefore, suppression of N-terminal-modifying enzymes, e.g., glutaminyl cyclase, which is capable of generating pGlu-Aβ peptides, leading to the dead-end of fast oligomer and fibril-forming Aβ species or upregulation of proteolytic enzymes should be considered when novel treatment strategies for neurodegenerative disorders are discussed (*40*).

ACKNOWLEDGMENT

We thank Dr. T. Hoffmann, H. Cynis, and Dr. J. Schilling for helpful discussions and technical support, as well as M. Gördes and D. Nowak for excellent technical support.

REFERENCES

1. Selkoe, D. J. (2001) Alzheimer's disease: Genes, proteins, and therapy, *Physiol. Rev. 81*, 741−766.
2. Esler, W. P., and Wolfe, M. S. (2001) A portrait of Alzheimer secretases—New features and familiar faces, *Science 293*, 1449−1454.
3. Gravina, S. A., Ho, L., Eckman, C. B., Long, K. E., Otvos, L., Jr., Younkin, L. H., Suzuki, N., and Younkin, S. G. (1995) Amyloid β protein (Aβ) in Alzheimer's disease brain. Biochemical and immunocytochemical analysis with antibodies specific for forms ending at Aβ40 or Aβ42(43), *J. Biol. Chem. 270*, 7013−7016.
4. Suzuki, N., Cheung, T. T., Cai, X. D., Odaka, A., Otvos, L., Jr., Eckman, C., Golde, T. E., and Younkin, S. G. (1994) An increased percentage of long amyloid β protein secreted by familial amyloid β protein precursor (β APP717) mutants, *Science 264*, 1336−1340.
5. Scheuner, D., Eckman, C., Jensen, M., Song, X., Citron, M., Suzuki, N., Bird, T. D., Hardy, J., Hutton, M., Kukull, W., Larson, E., Levy, L., Viitanen, M., Peskind, E., Poorkaj, P., Schellenberg, G., Tanzi, R., Wasco, W., Lannfelt, L., Selkoe, D., and Younkin, S. (1996) Secreted amyloid β-protein similar to that in the senile plaques of Alzheimer's disease is increased in vivo by the presenilin 1 and 2 and APP mutations linked to familial Alzheimer's disease, *Nat. Med. 2*, 864−870.
6. Jarrett, J. T., Berger, E. P., and Lansbury, P. T., Jr. (1993) The carboxy terminus of the β amyloid protein is critical for the seeding of amyloid formation: Implications for the pathogenesis of Alzheimer's disease, *Biochemistry 32*, 4693−4697.
7. McGowan, E., Pickford, F., Kim, J., Onstead, L., Eriksen, J., Yu, C., Skipper, L., Murphy, M. P., Beard, J., Das, P., Jansen, K., Delucia, M., Lin, W. L., Dolios, G., Wang, R., Eckman, C. B., Dickson, D. W., Hutton, M., Hardy, J., and Golde, T. (2005) Aβ42 is essential for parenchymal and vascular amyloid deposition in mice, *Neuron 47*, 191−199.
8. Iwatsubo, T., Saido, T. C., Mann, D. M., Lee, V. M., and Trojanowski, J. Q. (1996) Full-length amyloid-β(1−42(43)) and amino-terminally modified and truncated amyloid-β42(43) deposit in diffuse plaques, *Am. J. Pathol. 149*, 1823−1830.

9. Saido, T. C., Iwatsubo, T., Mann, D. M., Shimada, H., Ihara, Y., and Kawashima, S. (1995) Dominant and differential deposition of distinct β-amyloid peptide species, AβN3(pE), in senile plaques, *Neuron 14*, 457−466.
10. Sergeant, N., Bombois, S., Ghestem, A., Drobecq, H., Kostanjevecki, V., Missiaen, C., Wattez, A., David, J. P., Vanmechelen, E., Sergheraert, C., and Delacourte, A. (2003) Truncated β-amyloid peptide species in pre-clinical Alzheimer's disease as new targets for the vaccination approach, *J. Neurochem. 85*, 1581−1591.
11. Russo, C., Schettini, G., Saido, T. C., Hulette, C., Lippa, C., Lannfelt, L., Ghetti, B., Gambetti, P., Tabaton, M., and Teller, J. K. (2000) Presenilin-1 mutations in Alzheimer's disease, *Nature 405*, 531−532.
12. Russo, C., Saido, T. C., DeBusk, L. M., Tabaton, M., Gambetti, P., and Teller, J. K. (1997) Heterogeneity of water-soluble amyloid β-peptide in Alzheimer's disease and Down's syndrome brains, *FEBS Lett. 409*, 411−416.
13. Russo, C., Salis, S., Dolcini, V., Venezia, V., Song, X. H., Teller, J. K., and Schettini, G. (2001) Amino-terminal modification and tyrosine phosphorylation of [corrected] carboxy-terminal fragments of the amyloid precursor protein in Alzheimer's disease and Down's syndrome brain, *Neurobiol. Dis. 8*, 173−180.
14. Hosoda, R., Saido, T. C., Otvos, L. J., Arai, T., Mann, D. M., Lee, V. M., Trojanowski, J. Q., and Iwatsubo, T. (1998) Quantification of modified amyloid β peptides in Alzheimer disease and Down syndrome brains, *J. Neuropathol. Exp. Neurol. 57*, 1089−1095.
15. Harigaya, Y., Saido, T. C., Eckman, C. B., Prada, C.-J., Shoji, M., and unkin, S. G. (2000) Amyloid β protein starting pyroglutamate at position 3 is a major component of the amyloid deposits in the Alzheimer's disease brain, *Biochem. Biophys. Res. Commun. 276*, 422−427.
16. Saido, T. C., Yamao, H., Iwatsubo, T., and Kawashima, S. (1996) Amino- and carboxyl-terminal heterogeneity of β-amyloid peptides deposited in human brain, *Neurosci. Lett. 215*, 173−176.
17. Busby, W. H. J., Quackenbush, G. E., Humm, J., Youngblood, W. W., and Kizer, J. S. (1987) An enzyme(s) that converts glutaminyl-peptides into pyroglutamyl-peptides. Presence in pituitary, brain, adrenal medulla, and lymphocytes, *J. Biol. Chem. 262*, 8532−8536.
18. Fischer, W. H., and Spiess, J. (1987) Identification of a mammalian glutaminyl cyclase converting glutaminyl into pyroglutamyl peptides, *Proc. Natl. Acad. Sci. U.S.A. 84*, 3628−3632.
19. Schilling, S., Hoffmann, T., Manhart, S., Hoffmann, M., and Demuth, H. U. (2004) Glutaminyl cyclases unfold glutamyl cyclase activity under mild acid conditions, *FEBS Lett. 563*, 191−196.
20. Tekirian, T. L. (2001) Commentary: Aβ N-terminal isoforms: Critical contributors in the course of AD pathophysiology, *J. Alzheimer's Dis. 3*, 241−248.
21. He, W., and Barrow, C. J. (1999) The Aβ 3-pyroglutamyl and 11-pyroglutamyl peptides found in senile plaque have greater β-sheet forming and aggregation propensities in vitro than full-length Aβ, *Biochemistry 38*, 10871−10877.
22. Russo, C., Violani, E., Salis, S., Venezia, V., Dolcini, V., Damonte, G., Benatti, U., Arrigo, C., Patrone, E., Carlo, P., and Schettini, G. (2002) Pyroglutamate-modified amyloid β-peptides−AβN3-(pE)−strongly affect cultured neuron and astrocyte survival, *J. Neurochem. 82*, 1480−1489.
23. Piccini, A., Russo, C., Gliozzi, A., Relini, A., Vitali, A., Borghi, R., Giliberto, L., Armirotti, A., D'Arrigo, C., Bachi, A., Cattaneo, A., Canale, C., Torrassa, S., Saido, T. C., Markesbery, W., Gambetti, P., and Tabaton, M. (2005) β-Amyloid is different in normal aging and in Alzheimer disease, *J. Biol. Chem. 280*, 34186−34192.
24. Dahlgren, K. N., Manelli, A. M., Stine, W. B., Jr., Baker, L. K., Krafft, G. A., and LaDu, M. J. (2002) Oligomeric and fibrillar species of amyloid-β peptides differentially affect neuronal viability, *J. Biol. Chem. 277*, 32046−32053.
25. Chalifour, R. J., McLaughlin, R. W., Lavoie, L., Morissette, C., Tremblay, N., Boule, M., Sarazin, P., Stea, D., Lacombe, D., Tremblay, P., and Gervais, F. (2003) Stereoselective interactions of peptide inhibitors with the β-amyloid peptide, *J. Biol. Chem. 278*, 34874−34881.
26. Naiki, H., and Gejyo, F. (1999) Kinetic analysis of amyloid fibril formation, *Methods Enzymol. 309*, 305−318.
27. Kirkitadze, M. D., Condron, M. M., and Teplow, D. B. (2001) Identification and characterization of key kinetic intermediates in amyloid β-protein fibrillogenesis, *J. Mol. Biol. 312*, 1103−1119.
28. Balbach, J. J., Petkova, A. T., Oyler, N. A., Antzutkin, O. N., Gordon, D. J., Meredith, S. C., and Tycko, R. (2002) Supramolecular structure in full-length Alzheimer's β-amyloid fibrils: Evidence for a parallel β-sheet organization from solid-state nuclear magnetic resonance, *Biophys. J. 83*, 1205−1216.
29. Petkova, A. T., Ishii, Y., Balbach, J. J., Antzutkin, O. N., Leapman, R. D., Delaglio, F., and Tycko, R. (2002) A structural model for Alzheimer's β-amyloid fibrils based on experimental constraints from solid state NMR, *Proc. Natl. Acad. Sci. U.S.A. 99*, 16742−16747.
30. Sciarretta, K. L., Gordon, D. J., Petkova, A. T., Tycko, R., and Meredith, S. C. (2005) Aβ40-Lactam(D23/K28) models a conformation highly favorable for nucleation of amyloid, *Biochemistry 44*, 6003−6014.
31. Olofsson, A., Sauer-Eriksson, A. E., and Ohman, A. (2006) The solvent protection of alzheimer amyloid-β-(1-42) fibrils as determined by solution NMR spectroscopy, *J. Biol. Chem. 281*, 477−483.
32. Wood, S. J., Wetzel, R., Martin, J. D., and Hurle, M. R. (1995) Prolines and amyloidogenicity in fragments of the Alzheimer's peptide β/A4, *Biochemistry 34*, 724−730.
33. Pike, C. J., Overman, M. J., and Cotman, C. W. (1995) Amino-terminal deletions enhance aggregation of β-amyloid peptides in vitro, *J. Biol. Chem. 270*, 23895−23898.
34. Pike, C. J., Walencewicz, W., Kosmoski, J., Cribbs, D. H., Glabe, C. G., and Cotman, C. W. (1995) Structure-activity analyses of β-amyloid peptides: Contributions of the β 25−35 region to aggregation and neurotoxicity, *J. Neurochem. 64*, 253−265.
35. Miravalle, L., Calero, M., Takao, M., Roher, A. E., Ghetti, B., and Vidal, R. (2005) Amino-terminally truncated Aβ peptide species are the main component of cotton wool plaques, *Biochemistry 44*, 10810−10821.
36. Borghi, R., Patriarca, S., Traverso, N., Piccini, A., Storace, D., Garuti, A., Cirmena, G., Odetti, P., and Tabaton, M. (2006) The increased activity of BACE1 correlates with oxidative stress in Alzheimer's disease, *Neurobiol. Aging.*, in press.
37. Tomidokoro, Y., Lashley, T., Rostagno, A., Neubert, T. A., Bojsen-Moller, M., Braendgaard, H., Plant, G., Holton, J., Frangione, B., Revesz, T., and Ghiso, J. (2005) Familial Danish dementia: Coexistence of Danish and Alzheimer amyloid subunits (ADan and A{β}) in the absence of compact plaques, *J. Biol. Chem. 280*, 36883−36894.
38. Saido, T. C. (1998) Alzheimer's disease as proteolytic disorders: Anabolism and catabolism of β-amyloid, *Neurobiol. Aging 19*, S69−S75.
39. Stine, W. B., Jr., Dahlgren, K. N., Krafft, G. A., and LaDu, M. J. (2003) In vitro characterization of conditions for amyloid-β peptide oligomerization and fibrillogenesis, *J. Biol. Chem. 278*, 11612−11622.
40. Cynis, H., Schilling, S., Bodnár, M., Hoffmann, T., Heiser, U., Saido, T. C. and Demuth, H.-U. (2006) Inhibition of Glutaminyl Cyclase Alters Pyroglutamate Formation in Mammalian Cells, *Biochem. Biophys. Acta - Proteins and Proteomics*, doi: 10.1016/j.bbapap.2006.08.003.

BI0612667